

# Electrical and thermoelectric power properties of $\text{Cd}_{23}\text{Se}_{43}\text{S}_{34}$

S. EL-SAYED

*Physics Department, Faculty of Science, Al-Azhar University for Girls, Cairo, Egypt*

Electrical conductivity, I-V characteristics and thermoelectric power are investigated for  $\text{Cd}_{23}\text{Se}_{43}\text{S}_{34}$  film sample as a function of temperature and thickness. D.C conductivity increases with temperature, while it increases with increasing film thickness. The obtained results showed that the conduction activation energy has two values  $\Delta E_{\sigma_1}$  and  $\Delta E_{\sigma_2}$  indicating the presence of two different conduction mechanisms through the investigated range of temperature (327-400K). The thermopower (TEP) measurements carried out using differential dc method in the temperature range (322-370K) and the activation energy ( $\Delta E_s$ ) for TEP determined. Positive thermoelectric power suggests a large predominance of holes in electrical transport. The I-V characteristics of films are typical for a memory switch. The mean value of the threshold voltage  $V_{th}$  decreases with increasing temperature and increases with increasing film thickness. The switching voltage activation energy ( $\epsilon$ ) was determined. Agreement between the obtained value of ratio ( $\epsilon/\Delta E_{\sigma_2}$ ) with its values obtained theoretically on the basis of an electrothermal model was found.

(Received February 10, 2010; accepted March 12, 2010)

*Keywords:* Electrical conductivity; thermoelectric power; I-V characteristics;  $\text{Cd}_{23}\text{Se}_{43}\text{S}_{34}$  film, Chalcogenide

## 1. Introduction

Semiconducting glasses, namely Chalcogenide glasses, contain one or more of the Chalcogenide elements (group VI elements S, Se, Te) as alloy elements. They behave as semiconductors, more precisely; they exhibit amorphous semiconductor behavior with band gap energy from 1 to 3 eV. Chalcogenide glasses have received a lot of attention because they provide solid state physicists with new challenging fundamental problem and because of their possible technological applications [1, 2].

Certain amorphous semiconductors have shown interesting electrical effects involving a sudden change in resistance; these are generally grouped as switching properties. Typical materials which show these properties are the chalcogenide glasses [3]. It is now more than two decades since the first demonstration of switching and memory devices, based on chalcogenide glasses, were reported by Ovshinsky [4].

In this work, the electrical conductivity, thermoelectric power and I-V characteristics of amorphous  $\text{Cd}_{23}\text{Se}_{43}\text{S}_{34}$  films deposited on glass and pyrographite substrates were studied as a function of temperature and film thickness.

## 2. Experimental

Glassy alloy of  $\text{Cd}_{23}\text{Se}_{43}\text{S}_{34}$  was prepared by quenching technique. High purity (99.999%) materials are weighted according to their atomic percentage, and sealed in dry silica tube under a vacuum of  $10^{-5}$  torr. The ampoule is placed in the stable zone of an oscillatory furnace. The

ampoule temperature was raised to 119°C (m.p. of S) and kept constant for 2h, then it was raised to 220°C (m.p of Se) and kept constant for 2h, also it was raised to 320°C (m.p of Cd) and kept constant for 2h and finally it was raised to 700°C and kept constant for 6h. The oscillation of the tube was necessary to ensure homogenization of the composition obtained. The melt was quenched in ice-water.

Films with different thicknesses of  $\text{Cd}_{23}\text{Se}_{43}\text{S}_{34}$  were obtained by thermal evaporation under vacuum ( $10^{-6}$  torr using coating unit) on glass substrates for electrical and thermoelectric power measurements, and high polished pyrographite substrates for switching measurements. Film thickness was measured by Tolansky's interferometric method [5].

X-ray analysis was used to investigate the structure of the obtained material in film whose chemical composition was checked by energy dispersive analysis of X-ray (EDAX) (National Center of Radiation Research and Technology, Cairo, Egypt).

The two-probe method was used to measure the electrical conductivity, Ag metal used for electrodes. A digital electrometer (Keithley type 617A) using to measure the resistance of the film. A Chromel-Alumel thermocouple is fixed to the midpoint of the sample substrate to measure the film temperature.

Especially sample holder was used for the thermoelectric power measurements. The Al electrodes were deposited over the glass substrate to be used as electrodes. Differential heater, (Keithley type E 617A) used to measure the voltage ( $\Delta V$ ) across the sample resulting from the applied temperature gradient; the temperature difference ( $\Delta T$ ) between the limits of the

sample was measured by two calibrated Chromel-Alumel thermocouple mounted near the two electrodes.

Measurements of the current-voltage characteristics were carried out in a measuring cell fitted with two electrodes [6]. The lower one was made of copper in contact with the pyrographite substrate with dimensions  $(1.5 \times 0.8 \times 0.1 \text{ cm}^3)$ . The upper electrode was a movable platinum wire a thin circular and its diameter  $\approx 200 \mu\text{m}$ . Measurements were carried out using highly stabilized power supply (0-400 volt), a digital electrometer (Keithley type E617A) was used for the potential drop measurements and sensitive multimeter was used for the current measurements.

The experimental error during measurements was approximately  $\pm 2\%$ .

### 3. Results and discussion

#### 3.1 Structural properties

Fig. 1 shows the X-ray diffraction patterns for the investigated compositions  $\text{Cd}_{23}\text{Se}_{43}\text{S}_{34}$  film with two thickness  $\approx (600, 700 \text{ nm})$  as representative example. Detailed examination of the X-ray patterns indicate that all the films are amorphous with two main diffraction humps located at the same positions.

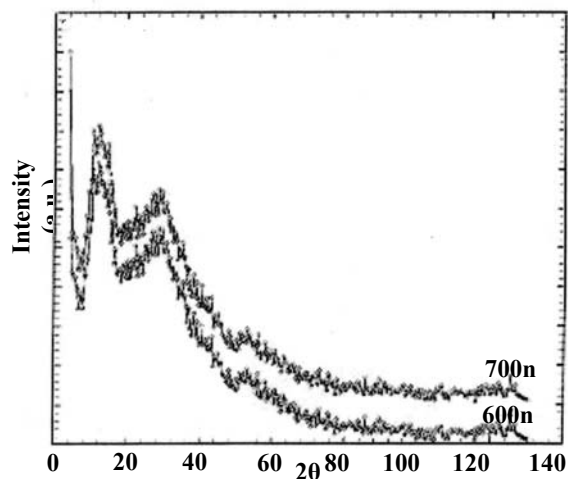
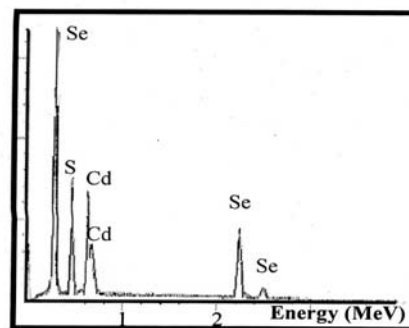


Fig. 1. The X-ray diffraction pattern for  $\text{Cd}_{23}\text{Se}_{43}\text{S}_{34}$  film.

The composition of the investigated films was checked using energy dispersive X-ray analysis (EDX). The obtained percentages of their constituent elements are illustrated in Fig. 2. They are close to the prepared compositions. Moreover, EDX analysis indicates the absence of impurities elements in the studied compositions.



$\text{Cd}_{23}\text{Se}_{43}\text{S}_{34}$

Fig. 2. The chemical composition of the obtained films is checked by (EDAX) energy dispersive analysis of X-ray  $\text{Cd}_{23}\text{Se}_{43}\text{S}_{34}$ .

#### 3.2 Electrical properties

The variation of electric conductivity  $\sigma$  with the reciprocal temperature in the temperature range (327-400K) for a  $\text{Cd}_{23}\text{Se}_{43}\text{S}_{34}$  films is displayed in Fig.(3) for films of different thickness in the range  $\approx (200-700 \text{ nm})$ . For all films, the electrical conductivity was found to be anegative exponential function of the absolute temperature according to the following relation [7].

$$\sigma = \sigma_0 \exp(-\Delta E_\sigma / k_B T), \quad (1)$$

where  $\sigma_0$  is the pre-exponential factor included charge carrier mobility and density of states,  $k_B$  the Boltzmann's constant,  $T$  the absolute temperature and  $\Delta E_\sigma$  the activation energy for conduction. As observed in Fig.(3) each obtained relation consists of two linear parts corresponding to lower (327-370K) and higher (370-400K) temperature ranges.

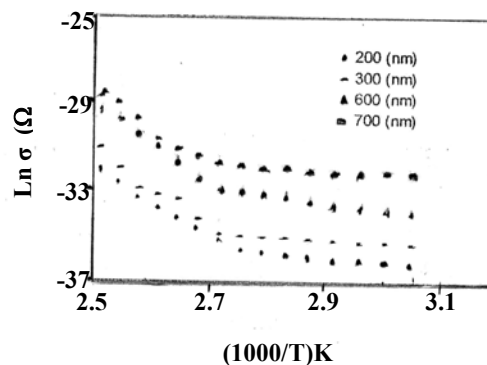


Fig. 3. Temperature dependence of the electrical conductivity for the composition  $\text{Cd}_{23}\text{Se}_{43}\text{S}_{34}$ .

The presence of two linear regions in the  $\ln \sigma$  vs  $1000/T$  plots is most likely due to the appearance of two conduction mechanism.

Values of  $\sigma_{RT}$  (room temperature conductivity) and  $\sigma_{01}$  for the investigated films with different thickness that estimated from Fig. 3 are given in Table 1. It is observed that the electrical conductivity at any temperature as well as  $\sigma_{RT}$  and  $\sigma_{01}$  increase with increasing film thickness in the investigated range  $\approx (200-700 \text{ nm})$ , which may be attributed to decrease in the degree of disorder and defects present in the structure [8].  $\Delta E_{\sigma_2}$  and  $\Delta E_{\sigma_1}$  are thickness slightly independent with values  $\approx 0.97$  and  $0.12 \text{ eV}$  for higher and lower temperature regions, respectively, since observed measured relations are parallel.

Table 1.

Thickness(nm)	$\sigma_{RT}$ ( $\Omega \text{ cm}$ ) <sup>-1</sup>	$\sigma_{01}$ ( $\Omega \text{ cm}$ ) <sup>-1</sup>
200	$9.2166\text{E}^{-15}$	1.1
300	$1.0877\text{E}^{-15}$	1.13
600	$2.1536\text{E}^{-14}$	1.15
700	$1.7241\text{E}^{-13}$	1.17

### 3.3 Thermoelectric power properties

The general expression for thermoelectric power (TEP) in the case of amorphous semiconductors has been discussed extensively in the literature [9,10]. In the case where carriers are excited to appropriate extended states beyond the mobility edges, or where charge carriers form small polarons and are transported by hopping near the band edges the expressions for TEP are formally identical. S is given by [10].

$$S = \pm \left( \frac{k}{e} \right) \left[ \left( \frac{\Delta E_s}{k_B T} \right) + A \right] \quad (2)$$

$$\Delta E_s = (E_F - E_V) \text{ or } (E_C - E_F) \quad (3)$$

where A is the small constant between 1 and 4[9] and represents the thermal energy transported by the carriers. Its magnitude is, therefore, dependent on the nature of the scattering processes. As already mentioned,  $\Delta E_s$  may be, in general, lower than  $\Delta E_{\sigma_2}$  and this difference is considered as equal to the mobility activation energy [9] or to the polaron-hopping barrier if the conduction is by small polarons [11].

Fig. 4 gives the temperature dependence of the thermo-electric power (S) for thin films of Cd<sub>23</sub>Se<sub>43</sub>S<sub>34</sub> at different temperature. As can be seen from Fig. 4 the (S) vs.  $1000/T$  graphs are straight lines with a positive slope indicating that (S) decreases linearly with temperature.

The activation energy ( $\Delta E_s$ ) has been calculated by using the slopes of Fig. 4 with value  $0.73 \text{ eV}$ , since observed measured relations are parallel. The temperature dependence of thermoelectric power (S) measures the energy difference between the Fermi level and the energy where charge transport occurs.

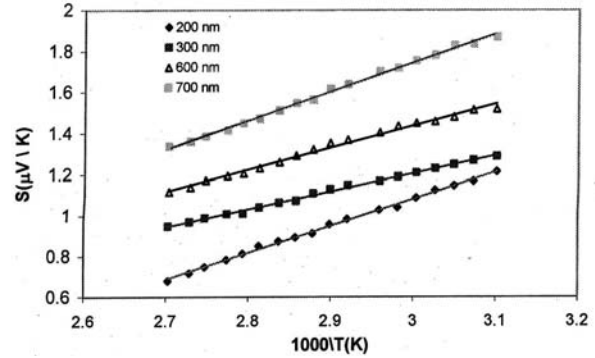


Fig. 4. The temperature dependence of the thermoelectric power for the compositions Cd<sub>23</sub>Se<sub>43</sub>S<sub>34</sub>.

In a simple one-band model with the Fermi energy pinned near the middle of the band gap, S is thermally activated with the activation energy of the carrier density activation energy. The difference between  $\Delta E_{\sigma_2}$  and  $\Delta E_s$  ( $0.23 \text{ eV}$ ) can be attributed to a mobility activation energy. The small polarons near the band edges may also contribute to the conductivity. These small polarons are usually associated with the structure of Se [12]. This results is in agreement with earlier estimates [13- 15].

### 3.4 I-V Characteristics

I-V characteristics curves were studied for Cd<sub>23</sub>Se<sub>43</sub>S<sub>34</sub> films of different thickness in the thickness range  $\approx (200,700 \text{ nm})$  at different temperature in the temperature range (323-353K). Fig.(5) shows room temperature I-V characteristics for Cd<sub>23</sub>Se<sub>43</sub>S<sub>34</sub> film with thickness 700nm as a representative example. It is observed that on increasing the applied voltage a very small current passes through the film, representing the OFF state (with the high resistance) of the switch. At certain applied voltage (called the threshold voltage  $V_{th}$ ) a sudden increase in current and drop in voltage take place. Further increase in the applied voltage increases the current passing through samples with any significant observed increase in the potential drop across sample, representing the ON state (with low resistance). On decreasing the applied voltage, current decreases reaching zero value and if the voltage is decreased and then increased, the I-V does not change, i.e. a permanent conduction state is established. This obtained I-V curves is typical for memory switching.

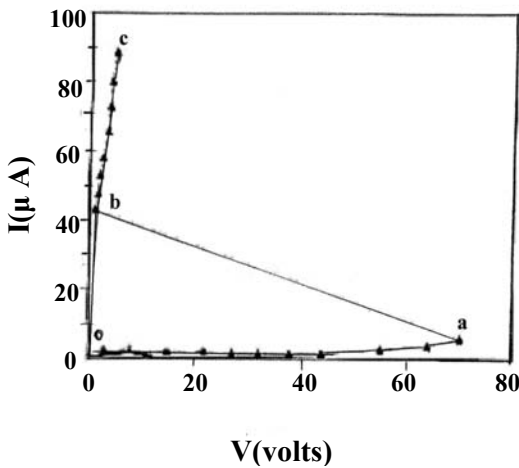


Fig. 5. Static I-V characteristic curve for  $Cd_{23}Se_{43}S_{34}$  thin film of thickness 700nm at room temperature.

The variation of the mean value of threshold voltage  $V_{th}$  for a  $Cd_{23}Se_{43}S_{34}$  films with thickness in the investigated range at room temperature was studied and illustrated in Fig. 6.

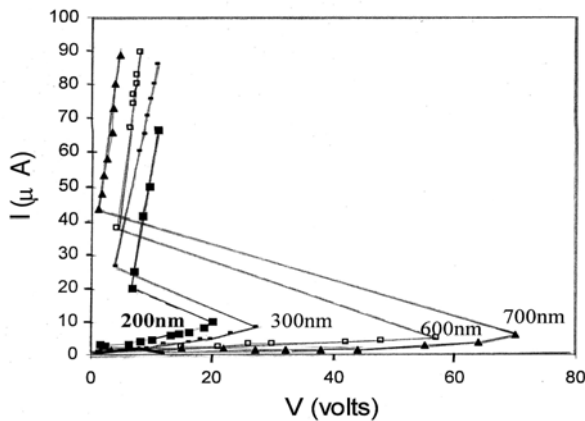


Fig. 6. Static I-V characteristic curve for  $Cd_{23}Se_{43}S_{34}$  film at different thickness (room temperature).

where  $V_{th}$  was measured for every film sample at different points uniformly distributed throughout the surface of the film and their mean values were calculated. A linear relationship between  $V_{th}$  and film thickness was obtained in the investigated range as in clear from Fig. 6. Observed relation of thickness dependence of  $V_{th}$  agrees with previous observation for different amorphous system [14-17].

The temperature dependence of the I-V characteristics for a  $Cd_{23}Se_{43}S_{34}$  films was studied in the temperature range (323-353K) for films with different thickness see from Fig. 7. The obtained I-V characteristics are also typical for the memory switching phenomenon with values of  $V_{th}$  decreases with increasing temperature.

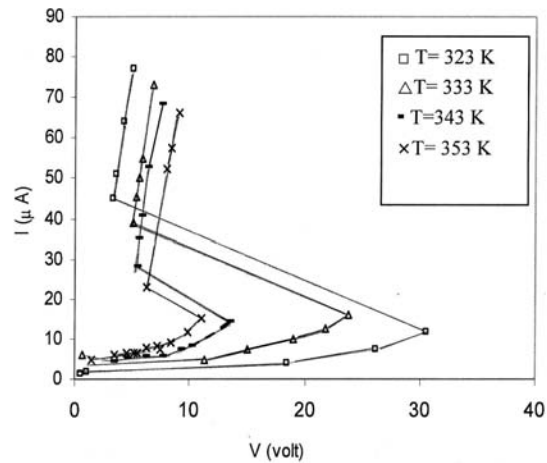


Fig. 7. Temperature dependence of  $V_{th}$  for the composition  $Cd_{23}Se_{43}S_{34}$  (thickness 600 nm).

The temperature dependence of  $V_{th}$  was plotted as  $\ln V_{th}$  vs  $1000/T$  as shown in Fig. 8 for thickness 600 nm as a representative curve. The obtained parallel straight lines satisfying the following equation [18]

$$V_{th} = V_0 \exp(\epsilon/k_B T), \quad (4)$$

where  $V_0$  is constant and  $\epsilon$  the threshold voltage activation energy.

The value of  $\epsilon$  that was calculated from the slope of the obtained line of Fig.(8) was found (0.49 eV) and independent on the thickness in the investigated range. The corresponding value of the ratio  $(\epsilon/\Delta E_{\sigma_2})$  was calculated also using values of  $\Delta E_{\sigma_2}$  obtained above. It is observed that the value of the ratio  $\epsilon/\Delta E_{\sigma_2}$  (0.50) is in good agreement with that obtained previously [14, 15, 17, 19, 20] for other amorphous semiconductors, as well as, with its value derived theoretically on the basis of an electrothermal model [18, 21] for the switching process.

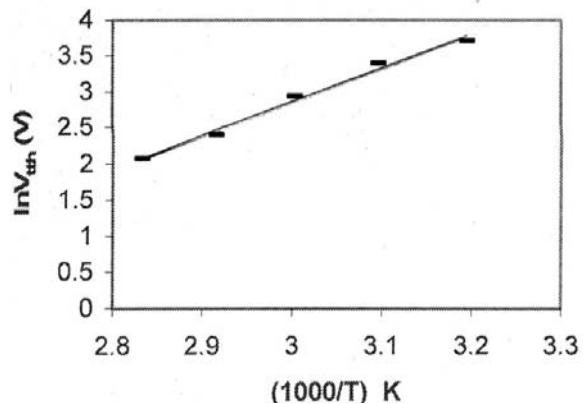


Fig. 8. Plot of  $\ln V_{th}$  vs.  $(1000/T)$  for the compositions  $Cd_{23}Se_{43}S_{34}$ .

So the observed temperature dependence of the threshold voltage for the pre-switching region can be explained in terms of an electrothermal model. The temperature of semiconductor is raised due to Joule heating. Since the conduction process in an amorphous material is of an activated type [22] the conduction of the sample is thus, increased when heated. This will allow more current flow through the heated region and allow more Joule-heating resulting in further increase in the current density. Stationary state is reached when the heat lost by conduction from the current filament becomes equal to the Joule-heat generated in that region.

The electrothermal model can be solved to a certain extent by finding a stationary state solution for the heat transport equation.

$$C(dT/dt)=\sigma E^2+\nabla(\psi\nabla T), \quad (5)$$

where C is the heat capacity,  $\psi$  is the thermal conductivity, E is the electrical field intensity ( $E=V_{th}/d$ ) and  $\sigma$  the electrical conductivity.

In the case of steady state breakdown, the time derivative of temperature (dT/dt) can be neglected for the solution of Eq. (5). Hence, the heat conduction equation for a small difference ( $\Delta T=T_m-T_s$ ) between the temperature at the middle of specimen  $T_m$  and that of the surface  $T_s$  gives [23].

$$8\psi(\Delta T/d^2)+\sigma E^2=0. \quad (6)$$

The steady state breakdown occurs when the amount of heat generated by Joule-heating cannot be removed by thermal conduction and the temperature difference necessary for breakdown can be obtained from Eqs. (5) and (6) in the form [18, 23].

$$\Delta T_{breakdown}=T^2k_B/\Delta E. \quad (7)$$

According to this equation  $\Delta T_{breakdown}$  was calculated for a- Cd<sub>23</sub>Se<sub>43</sub>S<sub>34</sub> films at different temperatures, and the obtained values are given in Table 2. This results is in agreement with previous observation for different amorphous system [14,15,17]. From the above results, it can be concluded that the observed memory type switching observed in Cd<sub>23</sub>Se<sub>43</sub>S<sub>34</sub> films could be satisfactory explained according to electothermal breakdown process.

Table 2. The breakdown characteristics as a function of temperature.

Temperature C <sup>0</sup>	$\Delta T_{breakdown}$
30	8.16
40	8.71
50	9.27
60	9.89
70	10.46
80	11.08

#### 4. Conclusions

Cd<sub>23</sub>Se<sub>43</sub>S<sub>34</sub> films were obtained by thermal evaporation technique on glass and pyrographite substrates. The obtained films are found to be of amorphous state. The electrical conductivity showed that the conduction activation energy has two values  $\Delta E_{\sigma_2}$  and  $\Delta E_{\sigma_1}$  which are thickness independent. I-V characteristics in Cd<sub>23</sub>Se<sub>43</sub>S<sub>34</sub> films are typical for a memory switch. The agreement between the obtained value of the ratio  $\varepsilon/\Delta E_{\sigma_2}$  (0.50) and its theoretically derived value (0.5) suggested that the switching phenomenon in Cd<sub>23</sub>Se<sub>43</sub>S<sub>34</sub> films can be explained according to an electrothermal model for the switching process.

#### References

- [1] J. G. Hernandez, E. L. Cruz, M. V. Limon, D. Strand, B. B. Chao, S. R. Ovshinsky, Solid State Commun. **95**, 593 (1995).
- [2] A. B. Seddon, J. Non-Cryst. Solids **184**, 44 (1995).
- [3] S. R. Ovshinsky, D. Alder, Disordered Materials Science and Technology, Amorphous Institute Press, New York, 1982.
- [4] S. R. Ovshinsky, Phys. Rev. Lett. **21**, 1450 (1968).
- [5] S. Tolansky, Multiple-beam Interference Microscopy of Metals, Academic Press, London, 1970.
- [6] M. A. Afifi, H. H. A. Labib, A. H. Abou El-Ela, K. A. Sharaf, Appl. Phys. A **46**, 113 (1988).
- [7] E. A. Davis, N. F. Mott, Phil. Mag. **22**, 903 (1970).
- [8] Z. S. El Mandouh, J. Appl. Phys. **78**, 7159 (1995).
- [9] H. Fritzsche. In Amorphous and Liquid Semiconductors. Edited by J. Tauc. Plenum Press, New York, 1971.
- [10] H. Fritzsche, Solid State Commun. **9**, 1813 (1971).
- [11] D. Amin, C. H. Seager, R. K. Quinn. Phys. Rev. Lett. **28**, 813(1972).
- [12] H. A. Vander plas, R. H. Bube. J. Non-Cryst. Solids **4**, 377 (1977).
- [13] Zishan H. Khan, M. Zulfeqaur, Arvind Kumar, M. Husain, Can. J. Phys. **80**, 19 (2002).
- [14] H. E. Atyia, Physica B **403**, 16 (2008).
- [15] M. A. Afifi, M. Fadel, E. G. El-Metwally, A. M. Shakra, Vacuum **77**, 256 (2005).
- [16] D. D. Thrbury, J. Non-Cryst. Solids, **11**, 113 (1972).
- [17] M. A. Afifi, A. E. Bekheet, N. A. Hegab, L. A., Wahab, J. Appl. Phys **40**, 133 (2007).
- [18] R. Mehra, R. Shyam, P. C. Mathur, J. Non-Cryst. Solids **31**, 435 (1979).
- [19] M. A. Afifi, N. A. Hegab, A. E. Bekheet, Vacuum **47**, 265 (1996).
- [20] G. A. Denton, G. M. Friedman, J. F. Schetzina, J. Appl. Phys. **46**, 3044 (1975).
- [21] K. W. Boer, S. R. Ovshinsky, J. Appl. Phys. **41**, 6 (1970).
- [22] A. H. Abou El-Ela, N. Abdel Mohsen, H. H. Labib, Appl. Phys. A **26**, 171 (1981).
- [23] K. Shimakova, Y. Inagaki, T. Arizami, Jpn. J. Appl. Phys. **12**, 1043 (1973).

\*Corresponding author: sozannasser@hotmail.com